Band manipulation and spin texture in interacting moiré helical edges

Yang-Zhi Chou, Jennifer Cano, and J. H. Pixley

Phys. Rev. B **104**, L201113 — Published 23 November 2021

DOI: 10.1103/PhysRevB.104.L201113

Band manipulation and spin texture in interacting moiré helical edges

Yang-Zhi Chou,[1,*] Jennifer Cano,[2,3] and J. H. Pixley[4,3,5]

[1] *Condensed Matter Theory Center and Joint Quantum Institute, Department of Physics, University of Maryland, College Park, Maryland 20742, USA*
[2] *Department of Physics and Astronomy, Stony Brook University, Stony Brook, New York 11974, USA*
[3] *Center for Computational Quantum Physics, Flatiron Institute, New York, New York 10010, USA*
[4] *Department of Physics and Astronomy, Center for Materials Theory, Rutgers University, Piscataway, NJ 08854 USA*
[5] *Physics Department, Princeton University, Princeton, New Jersey 08544, USA*

We develop a theory for manipulating the effective band structure of interacting helical edge states realized on the boundary of two-dimensional time-reversal symmetric topological insulators. For sufficiently strong interaction, an interacting edge band gap develops, spontaneously breaking time-reversal symmetry on the edge. The resulting spin texture, as well as the energy of the time-reversal breaking gaps, can be tuned by an external moiré potential (i.e., a superlattice potential). Remarkably, we establish that by tuning the strength and period of the potential, the interacting gaps can be fully suppressed and interacting Dirac points re-emerge. In addition, nearly flat bands can be created by the moiré potential with a sufficiently long period. Our theory provides a novel way to enhance the coherence length of interacting helical edges by suppressing the interacting gap. The implications of this finding for ongoing experiments on helical edge states is discussed.

Introduction. – Moiré heterostructures, such as magic-angle twisted bilayer graphene, provide tunable platforms to realize novel interaction-driven phases [1–36]. Microscopically, these interaction-driven phenomena result from extremely flat bands that are created by the relative twist of two-dimensional (2D) low-energy Dirac cones to a magic angle [37, 38], so that many body interactions become significant. Recent proposals have extended this paradigm to other 2D materials [39–49], unconventional superconductors [50, 51], ultracold atoms in optical lattices [52, 53], and acoustic metamaterials [54]. Engineering flat bands by tuning to a "magic angle" is quite general and may be induced by external quasiperiodic potentials and tunneling processes [55–59] that can be extended to a "magic-continuum" [60].

A moiré superlattice potential can also be used to control and manipulate a 2D Dirac cone on the surface of a topological insulator, producing favorable conditions to realize interacting instabilities such as topological superconductivity or quantum anomalous Hall by enhancing the density of states [61, 62]. However, if the surface states are protected by time-reversal symmetry, the formation of a flat, gapped, miniband is topologically obstructed. Spontaneous symmetry breaking permits an interaction-driven gap, but an analysis of the strong coupling regime is lacking.

In this letter, by focusing on the helical edge states of a 2D topological insulator, we utilize the power of bosonization to provide a clear theoretical demonstration of how strongly coupled interaction-driven phases emerge in moiré tuned topological edge states when time-reversal symmetry is spontaneously broken. In particular, we study the interplay between interactions and a moiré potential (specifically, a periodic potential in the continuum theory) on the 1D helical edge states of a 2D time-reversal-invariant topological insulator [63–78],

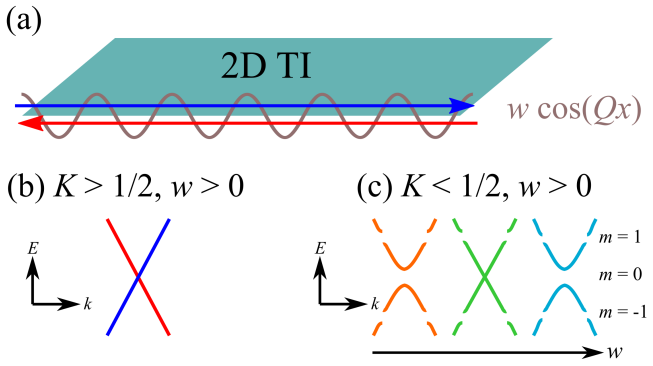

FIG. 1. Setup and band structure manipulation. (a) Illustration of the setup. A 2D TI edge state is perturbed by an external periodic potential, $V(x) = w\cos(Qx)$. (b) For a weak repulsive interaction ($1/2 < K < 1$), the edge band is unaffected by the external potential. (c) For a strong repulsive interaction ($K < 1/2$), interaction-induced gaps can open at both zero energy and finite energies. In addition, for particular w and Q, the interaction-induced gap may vanish, resulting in a re-emergent gapless edge (middle figure). The gaps are labeled by m corresponding to $E = mvQ/4$.

shown in Fig. 1(a). Distinct from previous works on the interaction-induced helical spin texture [79] and RKKY induced orders in the external spins [80, 81], we focus on the band dispersion of the strongly interacting edges, which can be manipulated by a time-reversal breaking gap at zero energy that develops due to interaction induced backscattering, i.e. umklapp processes [82, 83] [as sketched in Fig. 1(b) and (c)]. We show systematically that the spin textures of the interacting gaps can be controlled by both the oscillation period [79] and the amplitude of the periodic potential and exhibit a nontrivial structure. With the ability to manipulate the gaps in the band structure, we demonstrate that the edge band can be engineered such that re-emergent Dirac points and

nearly flat bands can be realized. The re-emergence of the Dirac point at $E = 0$ [Fig. 1(c)] indicates that the periodic potential can enhance the coherence length of the strongly interacting helical edge state, which is useful for ongoing experiments trying to observe topological insulator edge states in quantum wells [69–72, 84]. Our proposed set up depicted in Fig. 1(a) can also be realized in ultracold Fermi gases subjected to a two-dimensional spin orbit coupling [85, 86], where the edge potential can be generated via an additional one-dimensional optical lattice.

Model. – The edge of a 2D time-reversal-invariant topological insulator is described by a 1D Dirac Hamiltonian perturbed by interaction and an inhomogeneous potential[64, 82, 83],

$$\hat{H} = \sum_{r=R,L} \int dx \left[v_r \psi_r^\dagger \left(-i\partial_x \psi_r \right) + V(x) \psi_r^\dagger(x) \psi_r(x) \right] + U \int dx : \left[e^{i\delta G x} \left(\psi_L^\dagger \psi_R \right)^2 + \text{H.c.} \right] + \hat{H}_{LL} \tag{1}$$

where $v_r = \pm v_F$ is the Fermi velocity for $r = R/L$ and $\hat{H}_{LL}$ denotes the forward scattering interactions [87] whose precise form is not important here. In the above expressions ψ_R (ψ_L) is the right-moving (left-moving) fermionic field, $V(x)$ is a spatially varying potential, U encodes the interaction strength, $\delta G = 4k_F - G$, k_F is the Fermi wavevector, G is a reciprocal lattice vector, and $: \mathcal{O} :$ denotes the normal ordering of $\mathcal{O}$. The right-moving and the left-moving fermions form a Kramers pair. Under time-reversal, the fermionic fields are transformed as: $\psi_R \to \psi_L$, $\psi_L \to -\psi_R$, and $i \to -i$. Thus, time-reversal symmetry forbids elastic single-particle backscattering (e.g., $\psi_L^\dagger \psi_R$), but long-wavelength forward scattering (e.g., $\psi_R^\dagger \psi_R$) is allowed. In the presence of Rashba spin orbit coupling, the time-reversal symmetric backscattering interaction [U term in Eq. (1)] can arise, and spin is no longer a good quantum number. We focus only on $G = 0$ for simplicity, although the results do not rely on this assumption.

Thus, the interacting inhomogeneous helical edge can be described by $\hat{H} = \hat{H}_0 + \hat{H}_V + \hat{H}_U + \hat{H}_{\text{LL}}$ [88, 89]. To study the interplay between interactions and an external periodic potential, we consider

$$V(x) = w \cos(Qx), \tag{2}$$

where w controls the strength of the potential and $Q > 0$ dictates the oscillation in space. We assume that $2\pi/Q$ is not commensurate with the 2D lattice constant d. We also assume that the edge physics does not change the bulk topological phase.

Commensurate-incommensurate transitions.– The interacting helical fermions can be mapped to an interacting bosonic problem [87, 90] with two bosonic fields (ϕ and θ) that are related to the density and current operators of the original fermion degrees of freedom (see [91] for a detailed discussion.) To incorporate the effect of the external potential, we perform a linear transformation, $\theta'(x) = \theta(x) + \frac{Kw}{vQ} \sin(Qx)$, which yields the bosonized Hamiltonian

$$\hat{H}_b' = \int dx \frac{v}{2\pi} \left[K \left(\partial_x \phi \right)^2 + \frac{1}{K} \left(\partial_x \theta' \right)^2 \right] - \tilde{U} \int dx \cos\left[4\theta'(x) - \frac{4Kw}{vQ} \sin(Qx) + 4k_F x \right], \tag{3}$$

where v is the velocity of boson, K is the Luttinger parameter, $\tilde{U} = U/(2\pi^2 a^2)$[92], and a is the ultraviolet length scale in the low-energy theory. We focus only on repulsive interactions, corresponding to $K < 1$. Eq. (3) is the starting point of our work.

In the absence of the external potential (i.e., $w = 0$), the Hamiltonian in Eq. (3) maps to the Pokrovsky-Talapov model for the commensurate-incommensurate transition [87, 93]. At the Dirac point (i.e., $k_F = 0$), the model is commensurate, and the cosine term in Eq. (3) becomes relevant in the renormalization group sense, inducing a spectral gap for $K < 1/2$ [82, 83, 87]. For fillings that are sufficiently away from the Dirac point, the model is incommensurate, and the $\tilde{U}$ term is irrelevant, suggesting a Luttinger liquid behavior.

To study Eq. (3) with a nonzero w, we express the cosine term ($\tilde{U}$ term) as a Fourier series [94]:

$$\cos\left[4\theta'(x) - \frac{4Kw}{vQ} \sin(Qx) + 4k_F x \right] = \sum_{m=-\infty}^{\infty} |\tilde{F}_m| \cos\left[4\theta'(x) + (4k_F - mQ)x + \chi_m \right], \tag{4}$$

where $\tilde{F}_m$ corresponds to the Fourier component of $\exp\left[i \frac{4Kw}{vQ} \sin(Qx) \right]$ and χ_m is the phase of $\tilde{F}_m$. Intuitively, Eq. (4) shows that the presence of the potential has reorganized the interaction into a series of backscattering processes with momentum mQ, which, in conjunction with the Luttinger parameter, can each open a gap in the excitation spectrum. If such a gap, labelled by m, opens, then time reversal symmetry on the edge must be spontaneously broken, lifting the topological obstruction to a gapped boundary. In the following, we investigate Eqs. (3) and (4) by adopting the analysis in Refs. [95, 96], which considered a single cosine term ($w = 0$ case) [87, 93], to the case with multiple cosine terms ($w \neq 0$ case). As we will show, the gapped edge states exhibit a nontrivial magnetic structure. Further, the magnitude of the gap can be tuned by the strength and period of the potential, allowing a gapless Dirac cone to be realized at special points in the phase diagram.

The commensuration condition for each m [i.e. each cosine term in the summand of Eq. (4)] is $4k_F = mQ$. If this condition is satisfied, the $\tilde{F}_m$ term in Eq. (4) can open a band gap of size $2v\delta Q_c^{(m)}$ for sufficiently strong

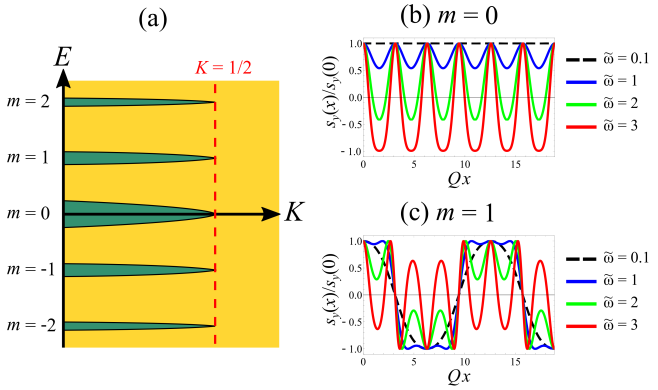

FIG. 2. Phase diagram and spin texture of the time-reversal breaking order. (a) The phase diagram for $|Q| > 4\delta Q_c^{(m)}$ based on bosonization analysis. The yellow region denotes the metallic phase. For $K < 1/2$, time-reversal breaking gaps (green regions) can be induced by the interaction. The energy of the gap is $E = mvQ/4$ for an integer m. The half width of the gap is $v\delta Q_c^{(m)}$, as discussed in the main text. (b)-(c): Normalized $s_y(x)$ [Eq. (6)] as a function of Qx. The phase shift $\zeta_{m,N}$ is set to zero for convenience. (b) $m = 0$. (c) $m = 1$. We define the dimensionless parameter $\tilde{\omega} = \frac{2Kw}{vQ}$. In both figures, $\tilde{\omega} = 0, 1, 2, 3$ correspond to the black dashed lines, blue lines, green lines, and red lines respectively.

interaction ($K < 1/2$), as shown in Fig. 2(a). The gapless state will be restored by sufficiently large incommensuration $|4k_F - mQ| > \delta Q_c^{(m)}$ as the integral over the cosine term in Eq. (3) for this m will vanish. In general, the threshold of commensuration, $\delta Q_c^{(m)}$, is a complicated function of $\tilde{U}$, w and K [87, 93]. If, for each m, $Q > 4\delta Q_c^{(m)}$, then the interacting gaps in the TI edge spectrum are well separated and we can treat the summand of Eq. (4) as a collection of independent cosine terms. On the other hand, if $Q \leq 4\delta Q_c^{(m)}$, the cosine terms in Eq. (4) interfere with each other; shortly we will employ an exact mapping at $K = 1/4$ to study this case.

Interacting gaps and spin texture. – For a helical edge state with $K < 1/2$, the commensurate cosine term (i.e., satisfying $|4k_F - mQ| < \delta Q_c^{(m)}$) in Eq. (4) becomes relevant, implying the formation of time-reversal breaking gaps at the energies $E(m) = mvQ/4$ labelled in Fig. 1(c). A phase diagram is illustrated in Fig. 2(a). Since the helical edge state is "spin-momentum locked," the time-reversal breaking gaps carry nontrivial magnetic structures. We discuss the alternative charge picture in [91].

To understand the consequence of spin momentum locking on the magnetic texture of each gap we compute the spin densities $\langle s_x(x)\rangle$ and $\langle s_y(x)\rangle$ (see [91] for definitions). When the backscattering interaction dominates (i.e., $K < 1/2$ and commensurate), we employ a mean field approach: for each mode m in Eq. (4), we solve for $\theta'(x)$ by minimizing the corresponding cosine term and then use $\theta'(x) = \theta(x) + \frac{Kw}{vQ}\sin(Qx)$ to compute the expectation values of s_x and s_y, yielding

$$\langle s_x(x)\rangle \approx \frac{1}{\pi a}\sin\left[\frac{mQx}{2} - \frac{2Kw}{vQ}\sin(Qx) + \zeta_{m,N}\right], \quad (5)$$

$$\langle s_y(x)\rangle \approx \frac{1}{\pi a}\cos\left[\frac{mQx}{2} - \frac{2Kw}{vQ}\sin(Qx) + \zeta_{m,N}\right], \quad (6)$$

where $\zeta_{m,N} = \pi N - \chi_m/2$ is an unimportant phase factor with arbitrary integer N. The expressions in Eqs. (5) and (6) reduce to a single frequency oscillation [79] in the limit $2Kw/(vQ) \ll 1$. Generically, the SDW states manifest non-sinusoidal oscillations due to the potential in Eq. (2). As plotted in Figs. 2(b) and (c), the value of w controls the spin texture of the time-reversal breaking order nontrivially, resulting in unusual spin order. In particular, the ferromagnetic order at $E = 0$ (equivalently $m = 0$) can be deformed to a qualitatively different finite-momentum SDW state in the presence of a sufficiently large w.

Luther-Emery theory and tunable band structure. – To go beyond the mean field approximation, we turn to the exact Luther-Emery refermionization mapping at $K = 1/4$ [87]. The interacting bosonized Hamiltonian in Eq. (3) maps to a noninteracting massive fermion Hamiltonian:

$$\hat{H}_b \to \sum_{r=R,L}\int dx\left[\tilde{\Psi}_r^\dagger\left(-i\tilde{v}_r\partial_x + \tilde{V}(x)\right)\tilde{\Psi}_r - \tilde{M}_r\tilde{\Psi}_{\bar{r}}^\dagger\tilde{\Psi}_r\right] \quad (7)$$

where $\tilde{v}_r = \pm v$ for $r = R/L$ is the velocity of the Luther-Emery fermions, $\tilde{V}(x) = V(x)/2 + vk_F/2$, $\tilde{M}_r = \pm iM$ for $r = R/L$, $M = U/(2\pi a)$, $\bar{r}$ denotes the opposite direction of r, and the Luther-Emery fermionic field is given by $\tilde{\Psi}_{R/L} = \frac{1}{\sqrt{2\pi a}}e^{i[\phi/2\pm 2\theta]}$. The mass term of the Luther-Emery fermions arises from the backscattering interaction [U term in Eq. (1)]. The Luther-Emery fields (Ψ_R and Ψ_L) are not simply related to the physical low-energy fermions (R and L). Nevertheless, we can extract information from the Luther-Emery theory such as the energy spectrum, density, and current [88].

For the Luther-Emery fermions, the band gap induced by spontaneous time-reversal symmetry breaking is $2|M|$. The appearance of finite-energy gaps [see Figs. 1(c) and 2(a)] can be understood intuitively by the band folding due to $V(x)/2$ and second order perturbation theory in $V(x)/2$. Note that the gap opening condition corresponds to $4k_F - mQ = 0$ with an integer m, which is consistent with the commensurate condition discussed previously.

In addition, controlling the magnitude of the periodic potential can close/reopen the zero-energy and finite-energy gaps. To see this analytically, we treat the periodic potential as a perturbation and compute the renormalized velocity and effective mass, which we find to be

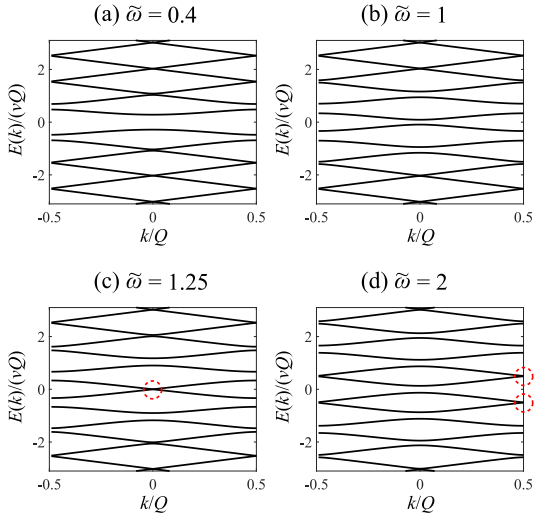

FIG. 3. Luther-Emery energy bands for $vQ = 3M$, varying $\tilde{\omega} = Kw/(vQ)$ (with $K = 1/4$). (a) $\tilde{\omega} = 0.4$ (b) $\tilde{\omega} = 1$ (c) $\tilde{\omega} = 1.25$ (d) $\tilde{\omega} = 2$. The Luther-Emery bands contain gaps due to spontaneous time-reversal symmetry breaking. The Dirac points at $k = 0$ and $k = \pm Q/2$ (circled by red dashed lines) are recovered for particular values of $\tilde{\omega}$ in (c) and (d).

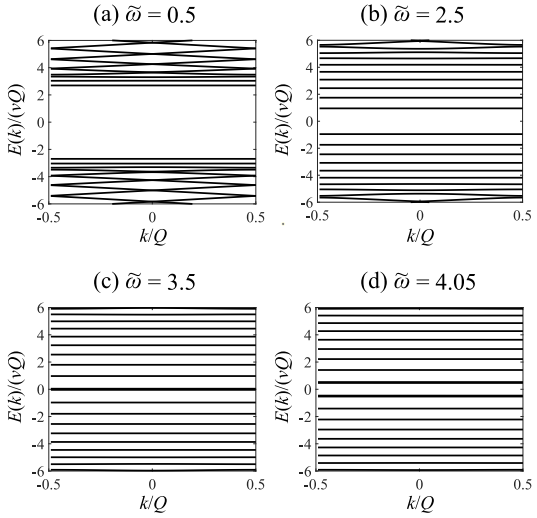

FIG. 4. Luther-Emery energy bands for $3vQ = M$, varying $\tilde{\omega} = Kw/(vQ)$ (with $K = 1/4$). (a) $\tilde{\omega} = 0.5$ (b) $\tilde{\omega} = 1$ (c) $\tilde{\omega} = 3.5$ (d) $\tilde{\omega} = 4.05$. The energy bands are nearly flat. The gap size at $E = 0$ depends on $\tilde{w}$. Nearly doubly degenerate zero energy bands emerge in (c). Similar nearly degenerate bands can also happen at finite energies as shown in (d).

given by

$$\tilde{v} = vZ\left[1 - \alpha^2 + \alpha^2 \frac{2v^2Q^2}{v^2Q^2 + M^2}\right], \; \tilde{M} = MZ\left(1 - \alpha^2\right), \tag{8}$$

respectively, where $Z = 1/(1+\alpha^2)$ is the wavefunction renormalization, and we have introduced a dimensionless coupling constant $\alpha^2 = \frac{w^2}{8(v^2Q^2+M^2)}$. Remarkably, the Dirac mass can be renormalized to zero (i.e. $\tilde{M} = 0$) when $\alpha = 1$, suggesting a Dirac point at $E = 0$ and band inversion signalled by the change in sign of $\tilde{M}$. This is rather interesting as it implies not only can the Dirac point re-emerge but this process has the potential to drive topological transitions on the edge. We confirm the perturbative analysis by numerically solving Eq. (7), shown in Fig. 3, where we plot the energy bands for a few representative values of w, demonstrating the re-emergence of Dirac points at zero energy [Fig. 3(c)] and finite energies [Fig. 3(d)].

For $vQ < |M|$, the low-energy bands can become nearly flat. Because of the narrow bandwidth in the low-energy minibands, perturbation theory cannot easily capture the qualitative features in this limit. We present numerical results in Fig. 4. Interestingly, we still find the gap closing for particular values of w as shown in Figs. 4(c) and (d). In summary, the periodic potential provides a nontrivial way to manipulate the edge bands, giving rise to finite-energy gaps, flat bands, and re-emergent Dirac points.

Implication for experiments. – Our theory describes a novel way to manipulate the emergent spin texture and edge state dispersion by an external periodic potential, $V(x) = w\cos(Qx)$, for the strongly interacting TI edges state ($K < 1/2$). The existence of novel SDW states is a manifestation of the spin-momentum locking in the helical edges. Based on our prediction, the spin texture can be controlled by both Q and w, and the predicted results in Eqs. (5) and (6) can be tested by scanning SQUID experiments on quantum wells [97, 98].

Our results also predict that the edge states can be driven through their own topological transition due to a band inversion. The stability of the bulk gap as the topological edge states are manipulated in such a fundamental way can be investigated using an ultracold Fermi gas with a two-dimensional spin orbit coupling, where both the stability of the bulk gap and the sensitivity to the edge gap can be seen through radiofrequency spectroscopy measurements of the spectral function [99, 100].

Now, we discuss how our setup can enhance edge state coherence in strongly interacting TI materials. A TI edge state with $K < 1/2$ can develop a gap at $E = 0$ due to spontaneous time-reversal symmetry breaking [82, 83], causing the edge state to become insulating at $E = 0$. For finite energies away from the interacting gap, chemical potential disorder generically induces localization in a 1D massive Dirac model [88, 101], destabilizing the quantized edge state conduction [69, 70, 72, 84]. Our work provides a possible resolution to such an almost inevitable scenario for strongly interacting TI edge states. As shown in Fig. 3 and Fig. 4, in the presence of a periodic potential, the magnitude of the gap depends on both Q and w; for appropriate parameters, the gap can be completely suppressed, revealing a re-emergent Dirac

point. Although such parameters are finely tuned, we have shown that in general, the interacting gap at $E = 0$ is reduced in the presence of the potential. Since the transport coherence length (defined by the length scale at which dissipationless edge states break down) increases as the gap decreases, this implies that the coherence length of strongly interacting helical edge states can be enhanced by an external periodic potential. When the coherence length is much larger than the system size, nearly quantized transport will result.

Thus, our work implies that a periodic potential at the edge of a 2D TI can lead to quantized transport even in the presence of interactions. Our proposal does not require precise information about the local potential landscape, in contrast to the gate training technique used in weakly interacting TI systems [102]. Since our theory describes interaction-driven edge phases, it is particularly relevant to 2D TI materials exhibiting strongly interacting edge states [69–72, 84].

Acknowledgments.– This work is supported by the Laboratory for Physical Sciences (Y.-Z.C.), by JQI-NSF-PFC (supported by NSF grant PHY-1607611, Y.-Z.C.). J.C. acknowledges the support of the Flatiron Institute and the Air Force Office of Scientific Research under Grant No. FA9550-20-1-0260. J.H.P is partially supported by the Air Force Office of Scientific Research under Grant No. FA9550-20-1-0136. The Flatiron Institute is a division of the Simons Foundation.

* yzchou@umd.edu

[1] Y. Cao, V. Fatemi, A. Demir, S. Fang, S. L. Tomarken, J. Y. Luo, J. D. Sanchez-Yamagishi, K. Watanabe, T. Taniguchi, E. Kaxiras, et al., Nature **556**, 80 (2018), URL http://dx.doi.org/10.1038/nature26154.

[2] Y. Cao, V. Fatemi, S. Fang, K. Watanabe, T. Taniguchi, E. Kaxiras, and P. Jarillo-Herrero, Nature **556**, 43 (2018), URL http://dx.doi.org/10.1038/nature26160.

[3] M. Yankowitz, S. Chen, H. Polshyn, Y. Zhang, K. Watanabe, T. Taniguchi, D. Graf, A. F. Young, and C. R. Dean, Science **363**, 1059 (2019).

[4] A. Kerelsky, L. J. McGilly, D. M. Kennes, L. Xian, M. Yankowitz, S. Chen, K. Watanabe, T. Taniguchi, J. Hone, C. Dean, et al., Nature **572**, 95 (2019).

[5] X. Lu, P. Stepanov, W. Yang, M. Xie, M. A. Aamir, I. Das, C. Urgell, K. Watanabe, T. Taniguchi, G. Zhang, et al., Nature **574**, 653 (2019).

[6] Y. Jiang, X. Lai, K. Watanabe, T. Taniguchi, K. Haule, J. Mao, and E. Y. Andrei, Nature **573**, 91 (2019).

[7] Y. Xie, B. Lian, B. Jäck, X. Liu, C.-L. Chiu, K. Watanabe, T. Taniguchi, B. A. Bernevig, and A. Yazdani, Nature **572**, 101 (2019).

[8] Y. Choi, J. Kemmer, Y. Peng, A. Thomson, H. Arora, R. Polski, Y. Zhang, H. Ren, J. Alicea, G. Refael, et al., Nature Physics **15**, 1174 (2019).

[9] H. Polshyn, M. Yankowitz, S. Chen, Y. Zhang, K. Watanabe, T. Taniguchi, C. R. Dean, and A. F. Young, Nature Physics **15**, 1011 (2019).

[10] Y. Cao, D. Chowdhury, D. Rodan-Legrain, O. Rubies-Bigorda, K. Watanabe, T. Taniguchi, T. Senthil, and P. Jarillo-Herrero, Phys. Rev. Lett. **124**, 076801 (2020), URL https://link.aps.org/doi/10.1103/PhysRevLett.124.076801.

[11] H. Polshyn, J. Zhu, M. A. Kumar, Y. Zhang, F. Yang, C. L. Tschirhart, M. Serlin, K. Watanabe, T. Taniguchi, A. H. MacDonald, et al., arXiv preprint arXiv:2004.11353 (2020).

[12] M. Serlin, C. Tschirhart, H. Polshyn, Y. Zhang, J. Zhu, K. Watanabe, T. Taniguchi, L. Balents, and A. Young, Science **367**, 900 (2020).

[13] A. L. Sharpe, E. J. Fox, A. W. Barnard, J. Finney, K. Watanabe, T. Taniguchi, M. Kastner, and D. Goldhaber-Gordon, Science **365**, 605 (2019).

[14] G. Chen, A. L. Sharpe, P. Gallagher, I. T. Rosen, E. J. Fox, L. Jiang, B. Lyu, H. Li, K. Watanabe, T. Taniguchi, et al., Nature **572**, 215 (2019).

[15] H. C. Po, L. Zou, A. Vishwanath, and T. Senthil, Phys. Rev. X **8**, 031089 (2018), URL https://link.aps.org/doi/10.1103/PhysRevX.8.031089.

[16] C. Xu and L. Balents, Physical review letters **121**, 087001 (2018).

[17] F. Wu, A. MacDonald, and I. Martin, Physical review letters **121**, 257001 (2018).

[18] M. Xie and A. H. MacDonald, Physical review letters **124**, 097601 (2020).

[19] Y.-H. Zhang, D. Mao, and T. Senthil, Phys. Rev. Research **1**, 033126 (2019), URL https://link.aps.org/doi/10.1103/PhysRevResearch.1.033126.

[20] B. Lian, Z. Wang, and B. A. Bernevig, Physical review letters **122**, 257002 (2019).

[21] F. Wu, E. Hwang, and S. Das Sarma, Phys. Rev. B **99**, 165112 (2019), URL https://link.aps.org/doi/10.1103/PhysRevB.99.165112.

[22] Y.-Z. You and A. Vishwanath, npj Quantum Materials **4**, 1 (2019).

[23] J. Kang and O. Vafek, Physical review letters **122**, 246401 (2019).

[24] N. Bultinck, E. Khalaf, S. Liu, S. Chatterjee, A. Vishwanath, and M. P. Zaletel, Physical Review X **10**, 031034 (2020).

[25] F. Xie, Z. Song, B. Lian, and B. A. Bernevig, Physical review letters **124**, 167002 (2020).

[26] B. Lian, Z.-D. Song, N. Regnault, D. K. Efetov, A. Yazdani, and B. A. Bernevig, Phys. Rev. B **103**, 205414 (2021), URL https://link.aps.org/doi/10.1103/PhysRevB.103.205414.

[27] B. A. Bernevig, B. Lian, A. Cowsik, F. Xie, N. Regnault, and Z.-D. Song, Phys. Rev. B **103**, 205415 (2021), URL https://link.aps.org/doi/10.1103/PhysRevB.103.205415.

[28] F. Xie, A. Cowsik, Z.-D. Song, B. Lian, B. A. Bernevig, and N. Regnault, Phys. Rev. B **103**, 205416 (2021), URL https://link.aps.org/doi/10.1103/PhysRevB.103.205416.

[29] N. Bultinck, S. Chatterjee, and M. P. Zaletel, Physical review letters **124**, 166601 (2020).

[30] J. Wang, Y. Zheng, A. J. Millis, and J. Cano, Phys. Rev. Research **3**, 023155 (2021), URL https://link.aps.org/doi/10.1103/PhysRevResearch.3.023155.

[31] O. Vafek and J. Kang, Phys. Rev. Lett. **125**,

257602 (2020), URL https://link.aps.org/doi/10.1103/PhysRevLett.125.257602.
[32] B.-B. Chen, Y. Da Liao, Z. Chen, O. Vafek, J. Kang, W. Li, and Z. Y. Meng, arXiv preprint arXiv:2011.07602 (2020).
[33] T. Cea and F. Guinea, Physical Review B **102**, 045107 (2020).
[34] J. Wang, J. Cano, A. J. Millis, Z. Liu, and B. Yang, arXiv preprint arXiv:2105.07491 (2021).
[35] F. Wu and S. Das Sarma, Phys. Rev. Lett. **124**, 046403 (2020), URL https://link.aps.org/doi/10.1103/PhysRevLett.124.046403.
[36] Y. Alavirad and J. Sau, Phys. Rev. B **102**, 235123 (2020), URL https://link.aps.org/doi/10.1103/PhysRevB.102.235123.
[37] R. Bistritzer and A. H. MacDonald, Proc. Natl. Acad. Sci. **108**, 12233 (2011), ISSN 0027-8424, URL https://www.pnas.org/content/108/30/12233.
[38] J. M. B. Lopes dos Santos, N. M. R. Peres, and A. H. Castro Neto, Phys. Rev. B **86**, 155449 (2012), URL https://link.aps.org/doi/10.1103/PhysRevB.86.155449.
[39] Y. Tang, L. Li, T. Li, Y. Xu, S. Liu, K. Barmak, K. Watanabe, T. Taniguchi, A. H. MacDonald, J. Shan, et al., Nature **579**, 353 (2020).
[40] E. C. Regan, D. Wang, C. Jin, M. I. Bakti Utama, B. Gao, X. Wei, S. Zhao, W. Zhao, Z. Zhang, K. Yumigeta, et al., Nature **579**, 359 (2020).
[41] Y. Shimazaki, I. Schwartz, K. Watanabe, T. Taniguchi, M. Kroner, and A. Imamoğlu, Nature **580**, 472 (2020).
[42] L. Wang, E.-M. Shih, A. Ghiotto, L. Xian, D. A. Rhodes, C. Tan, M. Claassen, D. M. Kennes, Y. Bai, B. Kim, et al., Nat. Mater. **19**, 861 (2020).
[43] K.-T. Tsai, X. Zhang, Z. Zhu, Y. Luo, S. Carr, M. Luskin, E. Kaxiras, and K. Wang, arXiv preprint arXiv:1912.03375 (2019).
[44] Y. Cao, D. Rodan-Legrain, O. Rubies-Bigorda, J. M. Park, K. Watanabe, T. Taniguchi, and P. Jarillo-Herrero, Nature **583**, 215 (2020).
[45] G. W. Burg, J. Zhu, T. Taniguchi, K. Watanabe, A. H. MacDonald, and E. Tutuc, Phys. Rev. Lett. **123**, 197702 (2019).
[46] C. Shen, Y. Chu, Q. Wu, N. Li, S. Wang, Y. Zhao, J. Tang, J. Liu, J. Tian, K. Watanabe, et al., Nat. Phys. **16**, 520 (2020).
[47] X. Liu, Z. Hao, E. Khalaf, J. Y. Lee, Y. Ronen, H. Yoo, D. Haei Najafabadi, K. Watanabe, T. Taniguchi, A. Vishwanath, et al., Nature **583**, 221 (2020).
[48] H. Pan, F. Wu, and S. Das Sarma, Phys. Rev. Research **2**, 033087 (2020), URL https://link.aps.org/doi/10.1103/PhysRevResearch.2.033087.
[49] J. Zang, J. Wang, J. Cano, and A. J. Millis, arXiv preprint arXiv:2105.11883 (2021).
[50] O. Can, T. Tummuru, R. P. Day, I. Elfimov, A. Damascelli, and M. Franz, Nature Physics **17**, 519 (2021).
[51] P. A. Volkov, J. H. Wilson, and J. Pixley, arXiv preprint arXiv:2012.07860 (2020).
[52] A. González-Tudela and J. I. Cirac, Phys. Rev. A **100**, 053604 (2019), URL https://link.aps.org/doi/10.1103/PhysRevA.100.053604.
[53] X.-W. Luo and C. Zhang, Phys. Rev. Lett. **126**, 103201 (2021), URL https://link.aps.org/doi/10.1103/PhysRevLett.126.103201.
[54] S. M. Gardezi, H. Pirie, S. Carr, W. Dorrell, and J. E. Hoffman, 2D Materials **8**, 031002 (2021).
[55] Y. Fu, E. J. König, J. H. Wilson, Y.-Z. Chou, and J. H. Pixley, npj Quantum Materials **5**, 1 (2020).
[56] T. Salamon, A. Celi, R. W. Chhajlany, I. Frérot, M. Lewenstein, L. Tarruell, and D. Rakshit, Phys. Rev. Lett. **125**, 030504 (2020), URL https://link.aps.org/doi/10.1103/PhysRevLett.125.030504.
[57] T. Salamon, R. W. Chhajlany, A. Dauphin, M. Lewenstein, and D. Rakshit, Phys. Rev. B **102**, 235126 (2020), URL https://link.aps.org/doi/10.1103/PhysRevB.102.235126.
[58] Y.-Z. Chou, Y. Fu, J. H. Wilson, E. J. König, and J. H. Pixley, Phys. Rev. B **101**, 235121 (2020), URL https://link.aps.org/doi/10.1103/PhysRevB.101.235121.
[59] Y. Fu, J. H. Wilson, and J. Pixley, arXiv preprint arXiv:2003.00027 (2020).
[60] Z.-X. Luo, C. Xu, and C.-M. Jian, arXiv preprint arXiv:2104.02087 (2021).
[61] J. Cano, S. Fang, J. H. Pixley, and J. H. Wilson, Phys. Rev. B **103**, 155157 (2021), URL https://link.aps.org/doi/10.1103/PhysRevB.103.155157.
[62] T. Wang, N. F. Q. Yuan, and L. Fu, Phys. Rev. X **11**, 021024 (2021), URL https://link.aps.org/doi/10.1103/PhysRevX.11.021024.
[63] C. L. Kane and E. J. Mele, Phy. Rev. Lett. **95**, 146802 (2005).
[64] C. L. Kane and E. J. Mele, Phy. Rev. Lett. **95**, 226801 (2005).
[65] B. A. Bernevig and S.-C. Zhang, Phys. Rev. Lett. **96**, 106802 (2006), URL http://link.aps.org/doi/10.1103/PhysRevLett.96.106802.
[66] M. König, S. Wiedmann, C. Brüne, A. Roth, H. Buhmann, L. W. Molenkamp, X.-L. Qi, and S.-C. Zhang, Science **318**, 766 (2007).
[67] A. Roth, C. Brüne, H. Buhmann, L. W. Molenkamp, J. Maciejko, X.-L. Qi, and S.-C. Zhang, Science **325**, 294 (2009).
[68] I. Knez, R.-R. Du, and G. Sullivan, Phys. Rev. Lett. **107**, 136603 (2011), URL http://link.aps.org/doi/10.1103/PhysRevLett.107.136603.
[69] L. Du, I. Knez, G. Sullivan, and R.-R. Du, Phys. Rev. Lett. **114**, 096802 (2015), URL https://link.aps.org/doi/10.1103/PhysRevLett.114.096802.
[70] T. Li, P. Wang, H. Fu, L. Du, K. A. Schreiber, X. Mu, X. Liu, G. Sullivan, G. A. Csáthy, X. Lin, et al., Phys. Rev. Lett. **115**, 136804 (2015), URL https://link.aps.org/doi/10.1103/PhysRevLett.115.136804.
[71] L. Du, T. Li, W. Lou, X. Wu, X. Liu, Z. Han, C. Zhang, G. Sullivan, A. Ikhlassi, K. Chang, et al., Phys. Rev. Lett. **119**, 056803 (2017), URL https://link.aps.org/doi/10.1103/PhysRevLett.119.056803.
[72] T. Li, P. Wang, G. Sullivan, X. Lin, and R.-R. Du, arXiv preprint arXiv:1707.09024 (2017).
[73] S. Tang, C. Zhang, D. Wong, Z. Pedramrazi, H.-Z. Tsai, C. Jia, B. Moritz, M. Claassen, H. Ryu, S. Kahn, et al., Nature Physics **13**, 683 (2017).
[74] S. Wu, V. Fatemi, Q. D. Gibson, K. Watanabe, T. Taniguchi, R. J. Cava, and P. Jarillo-Herrero, Science **359**, 76 (2018).
[75] P. Chen, W. W. Pai, Y.-H. Chan, W.-L. Sun, C.-Z. Xu, D.-S. Lin, M. Chou, A.-V. Fedorov, and T.-C. Chiang, Nature communications **9** (2018).
[76] M. M. Ugeda, A. Pulkin, S. Tang, H. Ryu, Q. Wu, Y. Zhang, D. Wong, Z. Pedramrazi, A. Martín-Recio,

Y. Chen, et al., Nature communications **9**, 3401 (2018).
[77] F. Reis, G. Li, L. Dudy, M. Bauernfeind, S. Glass, W. Hanke, R. Thomale, J. Schäfer, and R. Claessen, Science **357**, 287 (2017).
[78] R. Stühler, F. Reis, T. Müller, T. Helbig, T. Schwemmer, R. Thomale, J. Schäfer, and R. Claessen, Nature Physics **16**, 47 (2020).
[79] X.-Q. Sun, S.-C. Zhang, and Z. Wang, Phys. Rev. Lett. **115**, 076802 (2015), URL https://link.aps.org/doi/10.1103/PhysRevLett.115.076802.
[80] C.-H. Hsu, P. Stano, J. Klinovaja, and D. Loss, Phys. Rev. B **97**, 125432 (2018), URL https://link.aps.org/doi/10.1103/PhysRevB.97.125432.
[81] O. M. Yevtushenko and A. M. Tsvelik, Phys. Rev. B **98**, 081118 (2018), URL https://link.aps.org/doi/10.1103/PhysRevB.98.081118.
[82] C. Wu, B. A. Bernevig, and S.-C. Zhang, Phys. Rev. Lett. **96**, 106401 (2006).
[83] C. Xu and J. E. Moore, Phys. Rev. B **73**, 045322 (2006).
[84] A. Bubis, N. Mikhailov, S. Dvoretsky, A. Nasibulin, and E. Tikhonov, arXiv preprint arXiv:2104.13300 (2021).
[85] L. Huang, Z. Meng, P. Wang, P. Peng, S.-L. Zhang, L. Chen, D. Li, Q. Zhou, and J. Zhang, Nature Physics **12**, 540 (2016).
[86] B. Song, L. Zhang, C. He, T. F. J. Poon, E. Hajiyev, S. Zhang, X.-J. Liu, and G.-B. Jo, Science advances **4**, eaao4748 (2018).
[87] T. Giamarchi, *Quantum physics in one dimension* (Oxford Science Publications, Oxford, 2004).
[88] Y.-Z. Chou, R. M. Nandkishore, and L. Radzihovsky, Phys. Rev. B **98**, 054205 (2018), URL https://link.aps.org/doi/10.1103/PhysRevB.98.054205.
[89] Y.-Z. Chou, Phys. Rev. B **99**, 045125 (2019), URL https://link.aps.org/doi/10.1103/PhysRevB.99.045125.
[90] R. Shankar, *Quantum Field Theory and Condensed Matter: An Introduction* (Cambridge University Press, Cambridge, 2017).
[91] See supplemental material.
[92] The minus sign in front of the U term is due to the bosonization convention used in this work [90].
[93] V. L. Pokrovsky and A. L. Talapov, Phys. Rev. Lett. **42**, 65 (1979), URL https://link.aps.org/doi/10.1103/PhysRevLett.42.65.
[94] As we can see in the Taylor expansion of $\exp\left[i\frac{4Kw}{vQ}\sin(Qx)\right]$, the Fourier spectrum is discrete with nonzero values at integer multiple of Q.
[95] J. Vidal, D. Mouhanna, and T. Giamarchi, Phys. Rev. Lett. **83**, 3908 (1999), URL https://link.aps.org/doi/10.1103/PhysRevLett.83.3908.
[96] J. Vidal, D. Mouhanna, and T. Giamarchi, Phys. Rev. B **65**, 014201 (2001), URL https://link.aps.org/doi/10.1103/PhysRevB.65.014201.
[97] K. C. Nowack, E. M. Spanton, M. Baenninger, M. König, J. R. Kirtley, B. Kalisky, C. Ames, P. Leubner, C. Brüne, H. Buhmann, et al., Nature materials **12**, 787 (2013).
[98] E. M. Spanton, K. C. Nowack, L. Du, G. Sullivan, R.-R. Du, and K. A. Moler, Phys. Rev. Lett. **113**, 026804 (2014), URL https://link.aps.org/doi/10.1103/PhysRevLett.113.026804.
[99] J. Gaebler, J. Stewart, T. Drake, D. Jin, A. Perali, P. Pieri, and G. Strinati, Nature Physics **6**, 569 (2010).
[100] V. V. Volchkov, M. Pasek, V. Denechaud, M. Mukhtar, A. Aspect, D. Delande, and V. Josse, Phys. Rev. Lett. **120**, 060404 (2018), URL https://link.aps.org/doi/10.1103/PhysRevLett.120.060404.
[101] M. Bocquet, Nuclear Physics B **546**, 621 (1999).
[102] L. Lunczer, P. Leubner, M. Endres, V. L. Müller, C. Brüne, H. Buhmann, and L. W. Molenkamp, Phys. Rev. Lett. **123**, 047701 (2019), URL https://link.aps.org/doi/10.1103/PhysRevLett.123.047701.